Conclusion

The optimum solution conditions for Eu(III) complexes with tridentate iminodiacetate (IDA) and methyliminodiacetate (MIDA) ligands were determined from the luminescence spectra. The maximum contribution of EuL_3^{3-} species to the species formation could be attained when the molar metal-to-ligand ratios are 1 : 5 for the Eu(III)/IDA solution and 1 : 4 for the Eu(III)/MIDA solution under mild alkaline condition. Though $Eu(IDA)_3^{3-}$ and $Eu(MIDA)_3^{3-}$ show a similarity in coordination geometry, a large difference in the oscillator strength was found for the $^5D_0 \rightarrow {}^7F_2$ transition in luminescence and the $^7F_0 \rightarrow {}^5D_2$ transition in absorption.

Acknowledgment. This work was supported by the Korean Science and Engineering Foundation (KOSEF 951-0302-019-2). JHB would like to acknowledge financial support from Anyang University.

References

1. Carnall, W. T. In *Handbook on the Physics and Chemisty of Rare Earths*; Gschneibner, K. A., Jr.; Eyring Le R., Ed.; North-Holland Publishing Co.: 1979; Vol. 3, Chapter 24.
2. Bünzli, J.-C. G. *Lanthanide Probes in Life, Chemical and Earth Sciences*; Bünzli, J.-C. G.; Choppin, G. R., Ed.; Elsevier: Amsterdam, Oxford, New York, Tokyo, 1989; Chapter 7.
3. Kim, J. G.; Yoon, S. K.; Kang, J. G. *Bull. Korean Chem. Soc.* **1996,** *17*, 854.
4. Devlin, M. T.; Stephens, E. M.; Richardson, F. S. *Inorg. Chem.* **1984,** *23*, 4607.
5. Kim, J. G.; Yoon, S. K.; Yun, S. S.; Kang, J. G. *Bull. Korean Chem. Soc.* **1992,** *13*, 54.
6. Jung, S. H.; Yoon, S. K.; Kim, J. G.; Kang, J. G. *Bull. Korean Chem. Soc.* **1992,** *13*, 650.
7. Lis, S.; Choppin, G. R. *J. Alloys. Comp.* **1995,** *225*, 257.
8. Elbanowski, M.; Hnatejko, Z.; Stryla, Z.; Lis, S. *J. Alloys. Comp.* **1995,** *225*, 515.
9. Martell, A. E.; Smith, R. M. *Critical Stability Constants*; Plenum Press: New York, London, 1974; Vol. 1.
10. Judd, B. R. *Phys. Rev.* **1962,** *127*, 750.
11. Ofelt, G. S. *J. Chem. Phys.* **1962,** *37*, 511.
12. Peacock, R. D. In *Structure and Bonding*; Dunitz, J. D. Ed.; Springer-Verlag: Berline Heidelberg, New York, 1975; Vol. 22, p 83.

Preparation and Photophysical Properties of 4-(9-Anthrylethenyl)-4'-methyl-2,2'-bipyridine and Its Ruthenium Bipyridyl Complex $[Ru(bpy)_2(t\text{-aemb})](PF_6)_2$†

Eun Young Bae and Eun Ju Shin*

Department of Chemistry, Sunchon National University, Sunchon 540-742, Korea
Received September 20, 1997

Trans-4-(9-anthrylethenyl)-4'-methyl-2,2'-bipyridine(t-aemb) and its bipyridyl Ru complex $[Ru(bpy)_2(t\text{-aemb})](PF_6)_2$ (bpy=2,2'-bipyridine) **1** have been prepared and their excited state properties have been studied. t-Aemb exhibits solvent-dependent fluorescence and efficient *trans* → *cis* photoisomerization. **1** shows very weak fluorescence and is photochemically reactive. Fluorescence is wavelength-dependent. While the excitation into the MLCT band makes the complex fluorescent, direct absorption by the t-aemb ligand leads to the photoreaction of t-aemb ligand and no fluorescence is observed. **1** is considered to behave in part as bichromophoric molecule in which $[Ru(bpy)_3](PF_6)_2$ and anthryl group are covalently linked by ethenyl linkage. Because anthryl moiety is not effectively conjugated with bipyridylethenyl moiety due to steric hindrance, weak fluorescence can be explained due to the efficient energy or electron transfer.

Introduction

Polypyridine ruthenium(II) complexes have been of considerable interest because of their photophysical, photochemical and electrochemical properties.[1-3] The excited state properties and redox behavior of polypyridine ruthenium(II) complexes are controlled by low-lying electronic levels which are ligand-dependent.[4-6] Therefore, the rational design of the ligand is required for them.[4-6] Red shift of the metal-to-ligand charge transfer (MLCT) bands can be obtained by using ligands with lower π^* levels, but nonradiative decay rate constants increases as the energy gap between the ground and excited states decreases.[7,8] Because of this effect, complexes with low energy visible absorption bands are weak emitters and have short-lived excited states. The decreased lifetimes limit their use as sensitizers in pho-

*To whom correspondence should be addressed.
† Dedicated to Prof. Sang Chul Shim at Korea Advanced Institute of Science and Technology on the occasion of his 60th birthday.

toinduced electron and energy transfer. Using more rigid or extensively conjugated ligands, the complexes are known to lead to extended lifetimes due to smaller change in equilibrium displacement between ground and excited state.

Strouse *et al.* has prepared the olefin-linked, bis-2,2'-bipyridine derivative *trans*-1,2-bis-(4-(4'-methyl)-2,2'-bipyridyl) ethene (bbpe) and its Ru or Os complexes such as $[Ru(dmb)_2(bbpe)](PF_6)_2$ (dmb is 4,4'-dimethyl, 2,2'-bipyridine) in order to investigate the influence of electronic delocalization in MLCT excited state.[5] They found evidence in their photophysical properties for delocalization and dramatically extended lifetimes.

In this paper, *trans*-4-(9-anthrylethenyl)-4'-methyl-2,2'-bipyridine(t-aemb), as another olefin-linked derivative of 2,2'-bipyridine substituted by 9-anthrylethenyl group (L) and the related $[Ru(bpy)_2(t\text{-}aemb)](PF_6)_2$ complex have been prepared and their photophysical properties have been studied in order to investigate the influence of electronic delocalization in MLCT excited state. $[Ru(bpy)_2(t\text{-}aemb)](PF_6)_2$ exhibits very weak fluorescence. We expected t-aemb as one of more rigid or extensively conjugated ligands, but t-aemb is not extensively conjugated because of steric hindrance between ethenic H and anthracenic H1/H8 (see Results and discussion). Assuming that $[Ru(bpy)_2(t\text{-}aemb)](PF_6)_2$ behaves in part as bichromophoric molecule in which $[Ru(bpy)_3](PF_6)_2$ and anthryl group are covalently linked by ethenyl linkage, because anthryl moiety is not effectively conjugated with bipyridylethenyl moiety due to steric hindrance, weak fluorescence can be explained due to the efficient energy transfer and/or electron transfer between two chromophores.

Recently, bichromophoric molecules containing quenchers[9~11] (electron-accepting or -donating moieties) convalently linked to Ru complex sensitizer by functionalization of the 2,2'-bipyridine ligands[12] has received attention. The study for a ruthenium tris(bipyridine) complex covalently linked to anthracene, $[Ru(dmb)_2(dmb\text{-}an)](PF_6)_2$ (dmb=4,4'-dimethyl, 2,2'-bipyridine and dmb-an=4-(9-anthrylethyl),4'-methyl-2,2'-bipyridine), has been reported.[13] Our complex is quite similar to the complex except that our complex has double bond in place of single bond linkage between bipyridyl moiety and anthracene moiety. At appropriate separation distance, the individual chromophores in the complex should retain their photophysical properties and yet efficient intramolecular energy transfer should occur between them. On irradiation of this Ru complex, the excited singlet Ru moiety decays to the excited triplet state through efficient intersystem crossing, and then triplet-triplet energy transfer from Ru moiety to anthracene chromophore occurs.

The effect of anthrylethenyl substituent incorporated to 2,2'-bipyridine ligand on the photophysical properties of $[Ru(bpy)_2(t\text{-}aemb)](PF_6)_2$ was investigated in comparison with the above mentioned systems.

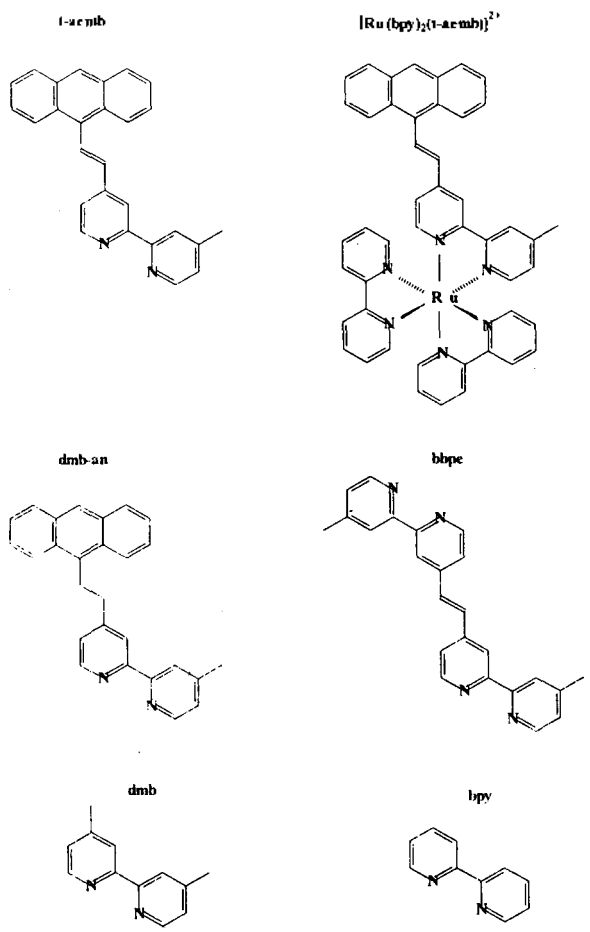

Scheme 1. Structures of $[(Ru(bpy)_2(t\text{-}aemb)]^{2+}$, t-aemb, and some other ligands.

Experimental

Materials

For spectroscopic measurements and photochemical reactions, n-hexane, tetrahydrofuran, ethyl acetate, acetonitrile, and methanol of HPLC grade (Merck) and ethanol of spectrophotometric grade (Aldrich) were used. Dichloromethane and toluene were freshly distilled from P_2O_5. Quinine sulfate (Aldrich), standard for fluorescence quantum yield measurement, was purified by recrystallization from water. Kiesel Gel 60 (70-230 mesh, Merck) was used for silica gel column chromatography, respectively. All other chemicals are used as received.

Synthesis

***Trans*-4-(9-anthrylethenyl)-4'-methyl-2,2'-bipyridine (t-aemb).** 9-Anthrylmethyltriphenylphosphonium bromide was prepared quantitatively by bromination of 9-methylanthracene in carbon tetrachloride using N-bromosuccinimide, followed by the reaction of triphenylphosphine in toluene. 4-(9-anthrylethenyl)-4'-methyl-2,2'-bipyridine(aemb) was synthesized by the Wittig reaction between 9-anthrylmethyltriphenylphosphonium bromide and 4'-methyl-2,2'-bipyridyl-4-carboxaldehyde[5] prepared from 4,4'-dimethyl-2,2'-bipyridine.[14] In dimethylsulfoxide (50 ml) solution of 9-anthrylmethyltriphenylphosphonium bromide (0.52 g, 1.0 mmol), sodium methoxide (0.05 g, 1.0 mmol) and 4'-methyl-2,2'-bipyridyl-4-carboxaldehyde (0.18 g, 0.9 mmol) were added and stirred at 100 °C for 3 hr. The resulting mixture was poured into distilled water, extracted three times with ethyl ether, rinsed several times with water, and dried with anhydrous magnesium sulfate. The resulting solution was concentrated in vacuo and was chromatographed on silica gel using dichloromethane as an eluent. The major fraction was evaporated and the resulting yellow solid (0.2 g, 60%

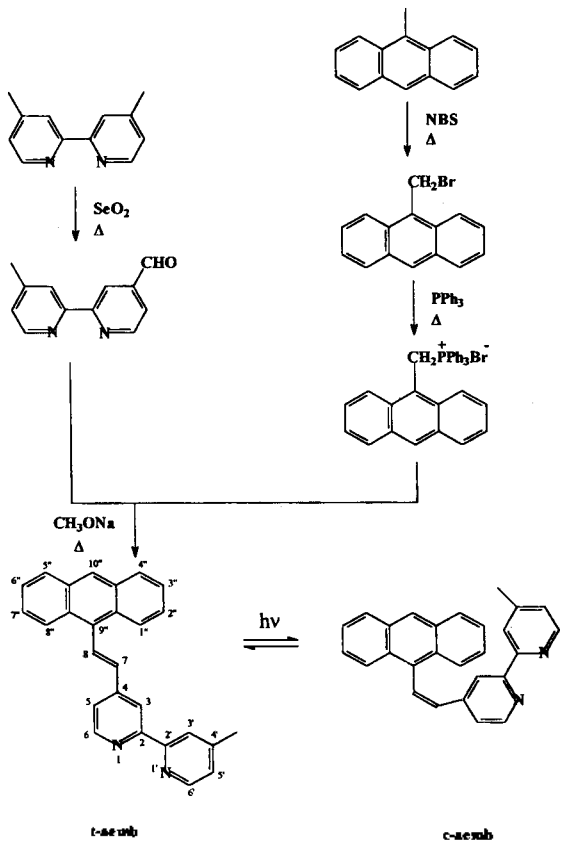

Scheme 2. Synthetic strategy for the preparation of t-aemb.

yield) was the mixture of *trans* and *cis* isomers of aemb which exhibited very similar retention times and could not be further separated. During the recrystallization with dichloromethane/*n*-hexane, the mixture converts to pure *trans* isomer. The precipitate was filtered and dried under vacuum. t-aemb is characterized by ^{1}H NMR, IR, UV, and mass spectral data. The ^{1}H NMR spectrum of the product obtained as yellow solid was consistent with the formation of a single *trans* isomer. IR: 3020, 1592, 1543, 1457, 1438, 1374, 742 cm^{-1}. ^{1}H NMR ($CDCl_3$): δ2.49 (3H, s, 4'-CH_3), 7.03 (1H, d, *J*=16.6 Hz, H8), 7.18 (1H, m, H6'), 7.48-7.52 (4H, m, H2", 3", 6", 7"), 7.55 (1H, dd, *J*=5.3, 1.6 Hz, H6), 8.03-8.06 (2H, m, H4", 5"), 8.28-8.35 (4H, m, H1", 8", 3', 7), 8.46 (1H, s, H10"), 8.59 (1H, d, *J*=4.8 Hz, H5'), 8.68 (1H, d, *J*=1.6 Hz, H3), 8.75 (1H, d, *J*=5.3 Hz, H5) ppm. EI-MS: m/e 355 [M-CH_3-2H]$^+$, 281 [M-terminal methylpyridyl ring+H]$^+$, 253, 207, 191, 167, 149.

Cis-4-(9-anthrylethenyl)-4'-methyl-2,2'-bipyridine(c-aemb). t-Aemb undergoes isomerization to c-aemb on UV irradiation of 350 nm after bubbling the solution using nitrogen. But, because *trans* and *cis* isomers exhibit very similar retention times, t-aemb and c-aemb was not able to be chromatographically separated. Photoisomerization of t-aemb to c-aemb was confirmed by the comparison of NMR data between the solution before and after irradiation. After irradiation of t-aemb for 1 hr, ratio of amount of *trans* to *cis* was estimated to about 1.01 : 1 from area of characteristic NMR peak corresponding to 4'-methyl proton substituted on bipyridine ring. ^{1}H NMR peaks of c-aemb was obtained from the difference between ^{1}H NMR peaks of the solution of t-aemb before and after irradiation. ^{1}H NMR ($CDCl_3$): δ 2.36 (3H, s, 4'-CH_3), 6.29 (1H, dd, *J*=1.6, 5.1 Hz, H8), 7.09 (1H, d, *J*=4.9, 1.0 Hz, H6'), 7.37-7.52 (5H, m, H6,2", 3", 6", 7"), 7.94 (1H, s, H3'), 7.95 (1H, d, *J*=5.1 Hz, H7), 8.02-8.06 (2H, m, H5', 4", 5"), 8.14-8.17 (2H, m, H1", 8"), 8.19 (1H, s, H10"), 8.47 (1H, s, H3), 8.50 (1H, d, *J*=4.9 Hz, H5) ppm.

Bis(2,2'-bipyridine)[*trans*-4-(9-anthrylethenyl)-4'-methyl-2,2'-bipyridine] ruthenium(II) hexafluorophosphate [(Ru(bpy)$_2$(t-aemb)](PF$_6$)$_2$]. Throughout the procedure below, room light was excluded. The complex $Ru(bpy)_2Cl_2$[14] (60 mg, 0.116 mmol) was added to ethylene glycol (30 ml) and heated at reflux for 30 min. The solution was cooled to room temperature, t-aemb (43 mg, 0.116 mmol) was added, and the mixture was heated at 110-120 °C in subdued light for 30 min. The solution was cooled to room temperature and diluted 1 : 1 with water and the excess aemb was removed by filteration. The product was precipitated by addition of a saturated aqueous solution of NH_4PF_6. The resulting powdery red-orange precipitate was filtered, washed with water and ether, and air-dried. [Ru(bpy)$_2$(t-aemb)](PF$_6$)$_2$ was obtained as a red-orange solid (92 mg, 0.085 mmol, 74%). IR: 1617, 1465, 842, 762, 557 cm^{-1}. ^{1}H NMR (DMSO-d_6): δ 2.56 (3H, s, 4'-CH_3), 7.18 (1H, d, *J*=16.5 Hz, H8), 7.41 (1H, d, *J*=5.7 Hz, H5'), 7.53-7.61 (9H, m, H2", 3", 6", 7", H5, bpy-H5, 5'), 7.70 (1H, d, *J*=5.7, H 6'), 7.76-7.81 (4H, m, bpy-H6, 6'), 7.94 (1H, d, *J*=5.1 Hz, H6), 8.16-8.24 (6H, m, H4", 5", bpy-H4, 4'), 8.36-8.39 (2H, m, H1", 8"), 8.67 (1H, s, H10"), 8.80-8.87 (5H, m, H7, bpy-H3, 3'), 8.92 (1H, s, H3'), 9.29 (1H, s, H3) ppm. FAB-MS: m/e 931 [M-PF$_6$]$^+$, 786 [M-2PF$_6$]$^+$.

Spectroscopic and photochemical measurements

^{1}H NMR spectra were obtained on 300 MHz Bruker DRX 300 spectrometer in chloroform-d_1 or dimethylsulfoxide-d_6. EI-Mass spectra were measured on Hewlett-Packard 5890 series II gas chromatograph-5972 series mass selective detector. Positive-ion fast atom bombardment mass spectrum was measured with Jeol HX 100/HX 110 Tandem mass spectrometer with sample mulled in 3-nitrobenzyl alcohol. FT-IR spectra were recorded in KBr pellets on Magna IR 550 spectrophotometer. The absorption spectra were recorded on a Hitachi U-321097 spectrophotometer. Electrochemical measurements were made using a Bioanalytical Systems (BAS) CV-50W potentiostat. Cyclic voltammetry was carried out in acetonitrile (0.1 M N(C_4H_9)$_4$(PF_6)) at 100 mV/s by using platinum counter electrode and glassy carbon working electrode, and all potentials were measured relative to an Ag/$AgNO_3$ (3 M KCl) reference electrode.

Aminco-Bowman Series 2 luminescence spectrometer was used for steady state fluorescence studies. SLM-AMINCO 48000S phase resolved spectrometer was used for measurement of fluorescence lifetime. Excitation wavelength at 360 nm for steady-state fluorescence of t-aemb, excitation wavelength at 360 nm and emission wavelength at 480 nm for fluorescence lifetime measurement, and irradiation wavelength of 350 nm for photoisomerization were employed in argon-saturated solution. Excitation wavelength at 460 nm for steady-state fluorescence of [Ru(bpy)$_2$(t-aemb)](PF$_6$)$_2$, excitation wavelength at 460 nm and emission wavelength at 640 nm for fluorescence lifetime measurement were employed in argon-saturated solution. For the

determination of quantum yield of fluorescence, concentrations of t-aemb and $[Ru(bpy)_2(t\text{-}aemb)](PF_6)_2$ were controlled to be ca. 1×10^{-5} M or below, where the absorbances of the solutions at the excitation wavelength (360 nm) were usually at a value of 0.07-0.08, in order to avoid inner filter effects and all the fluorescence spectra were corrected. The fluorescence quantum yields at room temperature were determined by three independent measurements using quinine sulfate in 0.1 N H_2SO_4 (Φ_f=0.55) for t-aemb and $[Ru(bpy)_3](PF_6)_2$ in acetonitrile (Φ_f=0.062) for Ru complex as standards.

Photolyses were conducted at 350 nm for t-aemb or 450 nm for $[Ru(bpy)_2(t\text{-}aemb)](PF_6)_2$ with Southern New England Rayonet Photochemical Reactor RPR 100 equipped with RMA-500 Merry-Go-Round Unit and sixteen RPR 3500 Å or 4500 Å fluorescent lamps. The samples were deoxygenated by purging with argon or nitrogen before irradiation. Photoreaction of t-aemb was monitored by absorption spectral changes and investigated by comparing the ^1H NMR spectra between before and after the photolysis.

Results and Discussion

Excited state properties of t-aemb. The absorption spectrum of t-aemb (Figure 1) is independent of solvent polarity and the absorption maximum in acetonitrile is 388 nm (ε=12,300), similar to those of *trans*-1-(9-anthryl)-2-phenylethene (t-9-APE)[15,16] and its aza-analogues (*trans*-1-(9-anthryl)-2-(n-pyridyl)ethene, t-n-APyE, n=2-4).[17]

The fluorescence spectrum of t-aemb at room temperature (Figure 1) exhibits strong dependence on the solvent polarity. As the solvent polarity is increased, the fluorescence maximum is red-shifted and the fluorescence quantum yield and lifetime is remarkably decreased, probably due to the intramolecular charge transfer, similar to t-4-APyE.[17] Absorption maxima and fluorescence maxima, quantum yields, and lifetimes of t-aemb in various solvents are represented in Table 1.

Table 1. Absorption maxima and fluorescence maxima, quantum yields and lifetimes for t-aemb in various solvents at room temperature and 77 K[a]

Solvent	E_T (30)	λ_a, nm	λ_f, nm	Φ_f	τ_f, ns
n-Hexane[b]	30.9	387	473	0.55	3.02
Toluene[b]	33.9	390	488	0.37	1.54
Tetrahydrofuran[b]	37.4	389	490	0.27	-
Ethylacetate[b]	38.1	388	488	0.22	-
Dichloromethane[b]	41.1	391	498	0.14	0.66
Acetonitrile[b]	46.0	388	500	0.07	0.13
Ethanol[b]	51.9	388	503	0.09	-
Methanol[b]	55.5	391	507	0.07	-
Methylcyclohexane[c]	31.2	-	453, 469	*ca.* 1	-
2-Methyltetrahydrofuran[c]	36.5	-	450, 469	*ca.* 1	-
Ethanol[c]	51.9	-	455, 468	*ca.* 1	-

[a]Excitation wavelength for fluorescence measurements is 360 nm. [b]At room temperature. [c]At 77 K.

t-Aemb is an aza-derivative of t-9-APE, which is well-known to carry out the photochemical *cis*→*trans* isomerization but not reverse reaction. Moreover, t-aemb has quite similar structure to t-4-APyE. Broad structureless fluorescence and large Stokes shift in t-aemb, as in t-9-APE[19] and t-4-APyE,[17] indicate nonplanarity in ground state molecules due to the steric strain. In the case of 9-APE,[19] its nonplanarity was supported by X-ray structural analyses.

Fluorescence of t-aemb is blue shifted on changing from room temperature to 77 K (Figure 2) and fluorescence maxima at 77 K (Table 1) are almost independent of solvent polarity similar to those of t-9-APE[19] and t-n-APyE.[17]

In contrast to parent hydrocarbon t-9-APE,[15,16,18,19] t-aemb undergoes isomerization to c-aemb on UV irradiation. This can be predictable from the fact that t-4-APyE[17] undergoes efficient photoisomerization in polar solvent and t-4-APyE

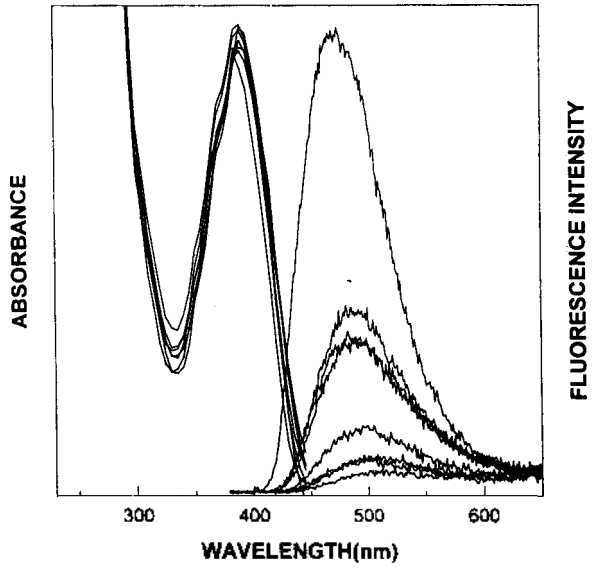

Figure 1. Absorption (left) and fluorescence (right) spectra of t-aemb in various solvents at room temperature. Absorption spectrum remains unchanged, but fluorescence is remarkably decreased with the solvent polarity.

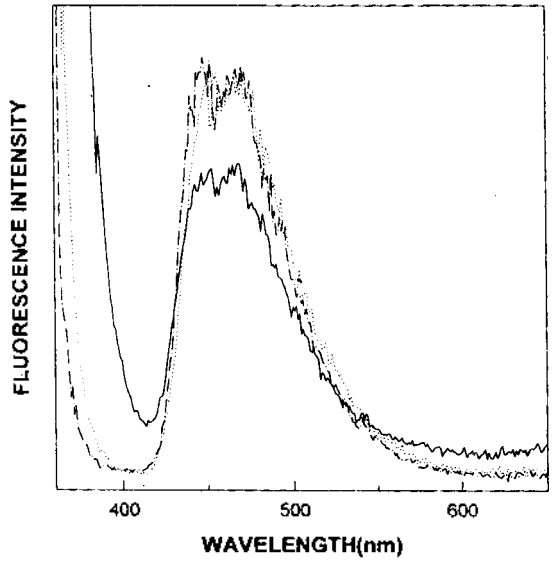

Figure 2. Fluorescence spectra of t-aemb in methylcyclohexane (solid line), 2-methyltetrahydrofuran (dot-dashed line), and ethanol (dotted line) at 77 K.

and t-aemb shows similar photophysical properties such as the solvent-dependent fluorescence. However, t-aemb and c-aemb were not able to be chromatographically separated, because *trans* and *cis* isomers exhibit very similar retention times. Photoisomerization of t-aemb to c-aemb was monitored by absorption spectral change (Figure 3). With the irradiation time, the absorption spectrum was more structured and blue shifted, similar to those of c-APE[19] and c-n-APyE.[17] As shown in Figure 3, irradiation for 1 hr leads to the photostationary state. The formation of c-aemb was further confirmed by the comparison of NMR data between the solution before and after irradiation (Figure 4). After irradiation (about 1 hr) of t-aemb until the solution reaches the photostationary state, ratio of the amount of *trans* to *cis* was estimated to about 1.01 : 1 from area of characteristic NMR peak corresponding to 4'-methyl proton substituted on bipyridine ring. ^{1}H NMR peaks of c-aemb were obtained from the difference between ^{1}H NMR peaks of the solution before and after irradiation as described in Experimental section.

Absorption and fluorescence spectra of [(Ru(bpy)$_2$(t-aemb)](PF$_6$)$_2$. The absorption spectrum of the complex [Ru(bpy)$_2$(t-aemb)](PF$_6$)$_2$ in acetonitrile is shown in Figure 5. The absorption bands are summerized in Table 2 and compared with those of the related Ru complexes.[5,6,13] The UV-vis absorption spectrum of [Ru(bpy)$_2$(t-aemb)](PF$_6$)$_2$ in acetonitrile is characterized, as for the other tris(bipyridyl) ruthenium(II) complexes, by intense ligand-centered π-π^* transitions in the UV and metal-to-ligand charge transfer (MLCT) transitions in the visible region.[1] On comparison of the absorption spectra of both [Ru(bpy)$_2$(t-aemb)](PF$_6$)$_2$ and [Ru(bpy)$_3$](PF$_6$)$_2$[1] (Figure 5), the bands at 288 nm can be assigned to bpy ligand-centered π-π^* transitions. Similarly, the band occurring at 461 nm are assigned to MLCT(d-π^*) transitions which are red-shifted relative to those reported for [Ru(bpy)$_3$](PF$_6$)$_2$ by the substitution of a anthrylethene moiety to the bpy fragment. While weak 244 nm band in [Ru(bpy)$_3$](PF$_6$)$_2$ is due to MLCT(d-π^*) transition,[1] strong 254 nm band of [Ru(bpy)$_2$(t-aemb)](PF$_6$)$_2$ is attributable to the aemb ligand (Figure 5). As t-aemb ligand is not planar

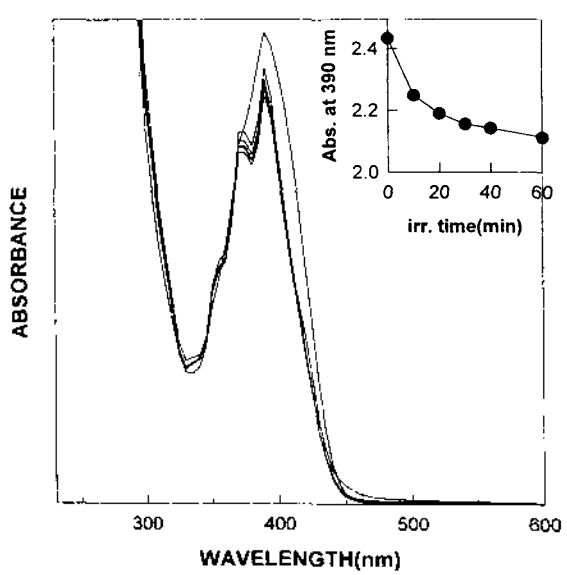

Figure 3. Absorption spectral change of t-aemb in dichloromethane on irradiation at 350 nm.

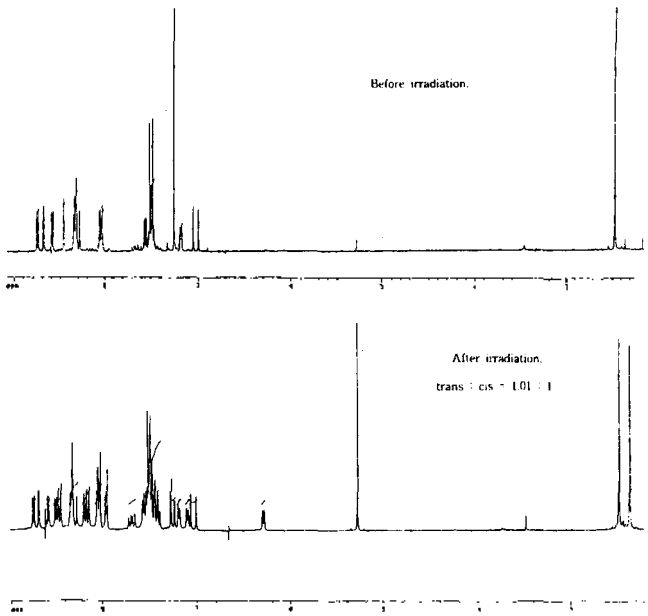

Figure 4. 300 MHz ^{1}H NMR spectra of t-aemb before irradiation (upper) and after irradiation (lower) at 350 nm in $CDCl_3$.

due to the steric repulsion as indicated above, the delocalization is not effective through the entire molecule. The possibility that [Ru(bpy)$_2$(mbpy)]$^{2+}$ (mbpy=4-methyl-2,2'-bipyridine) and anthracene connected by ethene bridge behave as two independent chromophores was examined by the absorption spectra. The absorption spectrum of the complex [Ru(bpy)$_2$(t-aemb)](PF$_6$)$_2$ is not exactly superimposed on the sum of the absorption spectra of [Ru(bpy)$_3$](PF$_6$)$_2$ and t-aemb, and the absorption band contributed by t-aemb is not easily distinguishable. This is in contrast to the facts that the absorption spectrum of the [Ru(dmb)$_2$(dmb-an)](PF$_6$)$_2$ where [Ru(dmb)$_3$](PF$_6$)$_2$ moiety and the covalently linked anthracene moiety behave two independent chromophores is superpos-

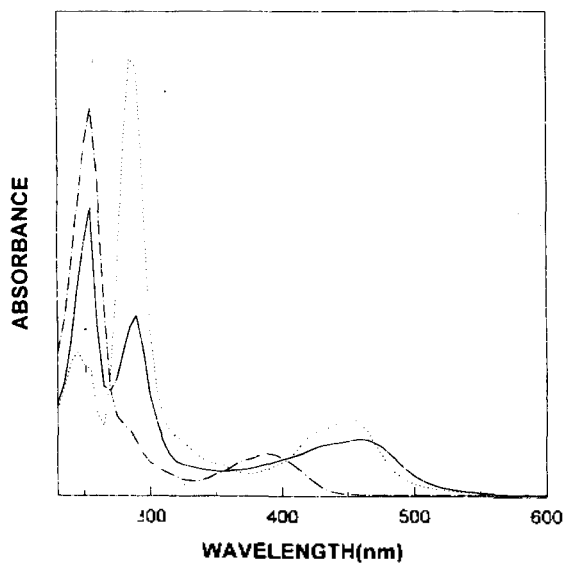

Figure 5. The absorption spectrum of [Ru(bpy)$_2$(t-aemb)](PF$_6$)$_2$ (solid line) in acetonitrile along with those of [Ru(bpy)$_3$](PF$_6$)$_2$ (dotted line) and t-aemb(dot-dashed line) in acetonitrile.

ed absorption spectra of the [Ru(dmb)$_3$](PF$_6$)$_2$ complex and the anthracene.[13] Moreover, the MLCT band of the complex [Ru(bpy)$_2$(t-aemb)](PF$_6$)$_2$ is red-shifted and broad relative to that of [Ru(bpy)$_3$](PF$_6$)$_2$. These indicate that, in the t-aemb ligand, bpy and anthracene do not behave two independent chromophores and some electronic interaction between two moieties is present.

Visible excitation into the MLCT band leads to room temperature photoluminescence in argon saturated acetonitrile. The complex [Ru(bpy)$_2$(t-aemb)](PF$_6$)$_2$ on the excitation at 460 nm exhibits broad, structureless fluorescence at room temperature, although no fluorescence is observed on the excitation at 360 nm. At 77 K, fluorescence is blue-shifted (from 643 to 590 nm) but still weak and typical MLCT vibronic structure was observed. The fluorescence spectra of [Ru(bpy)$_2$(t-aemb)](PF$_6$)$_2$ both at room temperature and 77 K were shown in Figure 6, for comparison, together with those of [Ru(bpy)$_3$](PF$_6$)$_2$. Excitation and absorption spectra are identical within experimental error indicating that the fluorescence arises from the complex but not the impurities. The emission maxima, quantum yields, and lifetimes for [Ru(bpy)$_2$(t-aemb)](PF$_6$)$_2$ and, for comparison purpose, for [Ru(bpy)$_3$](PF$_6$)$_2$,[6] [Ru(dmb)$_3$](PF$_6$)$_2$,[5] [Ru(dmb)$_3$](PF$_6$)$_2$,[5] [Ru(dmb)$_2$(bbpe)](PF$_6$)$_2$,[5] and [Ru(dmb)$_2$(dmb-an)](PF$_6$)$_2$[13] are collected in Table 2. The excitation wavelength at 460 nm was used for the fluorescence measurement. As shown in Figure 6, [Ru(bpy)$_2$(t-aemb)](PF$_6$)$_2$ (643 nm) in acetonitrile at room temperature emits at a longer wavelength than [Ru(bpy)$_3$](PF$_6$)$_2$ (626 nm), and has much smaller fluorescence quantum yield. Similarly, at 77 K in ethanol, [Ru(bpy)$_2$(t-aemb)](PF$_6$)$_2$ (585, 631, 690 nm) emits at a longer wavelength than [Ru(bpy)$_3$](PF$_6$)$_2$ (580, 624, 682 nm). The ratio of fluorescence quantum yields of [Ru(bpy)$_2$(t-aemb)](PF$_6$)$_2$ and [Ru(bpy)$_3$](PF$_6$)$_2$ is evaluated to be about 0.12 : 1 at 77 K, similar to the ratio (0.11 : 1) at room temperature. The relative luminescence quantum yields in acetonitrile follow the sequence [Ru(bpy)$_3$](PF$_6$)$_2$ > [Ru(bpy)$_2$(t-aemb)](PF$_6$)$_2$ > [Ru(dmb)$_2$(dmb-an)](PF$_6$)$_2$. In contrast to the expectation on comparison with [Ru(dmb)$_2$(bbpe)](PF$_6$)$_2$, which has been exhibited dramatically extended lifetimes by the influence of electronic delocalization in MLCT excited state, [Ru(bpy)$_2$(t-aemb)](PF$_6$)$_2$ shows very weak fluorescence and its fluorescence lifetime cannot be measured. This may be due to the efficient intramolecular energy transfer or electron transfer from Ru center to t-aemb moiety as in the reference complex [Ru(bpy)$_2$(bpy-an)](PF$_6$)$_2$ where intramolecular energy transfer occurred from Ru center to anthracene moiety. Assuming that [Ru(bpy)$_2$(t-aemb)](PF$_6$)$_2$ behaves in part as bichromophoric molecule in which [Ru(bpy)$_2$(mbpy)](PF$_6$)$_2$ and anthryl group is covalently linked by ethenyl linkage but anthryl moiety is not effectively conjugated with bipyridylethenyl moiety due to steric hindrance, weak fluorescence can be explained due to the efficient intramolecular energy or electron transfer.

Table 2. Absorption and fluorescence spectral data and electrochemical data for [Ru(bpy)$_2$(t-aemb)](PF$_6$)$_2$ in acetonitrile at room temperature in comparison with those for other Ru complexes[5,6,13]

Ru complex[a]	λ_a, nm (ε)	λ_f, nm	Φ_f	τ_f, ns	$E_{1/2}$[b], V Ox.	Red.
[Ru(bby)$_2$ (t-aemb)]$^{2+}$	461(16120) 449(15540) 440(14970) 288(50940) 254(80530)	643 (585, 631, 690)[d]	0.0066	-	+1.33	− 1.29 − 1.39 − 1.68
[Ru(bpy)$_3$]$^{2+}$	451(14000) 288(79500) 254(sh) (21400) 244(24400)	626 (579, 624, 682)[d]	0.062	920	+1.29	− 1.33 − 1.52 − 1.78
[Ru(dmb)$_3$]$^{2+}$	458(12650) 432(10500) 360(6040) 328(9950) 288(73100)	642	0.100	950	+1.13	− 1.45 − 1.64 − 1.88
[Ru(dmb)$_2$ (bbpe)]$^{2+}$	482(20300) 335(sh) 315(sh) 290(69000)	732	0.010	1150	+1.15	− 1.04 1.30 − 1.65
[Ru(dmb)$_2$ (dmb-an)]$^{2+}$	461(13500) 432(10500) 390 370 350	-	*ca.* 0	-	-	-

[a]PF$_6$ salt. [b]In acetonitrile (0.1 M NEt$_4$BF$_4$). [c]Excitation wavelength for fluorescence measurement is 460 nm. [d]At 77 K.

Electrochemical studies. The electrochemical behavior of polypyridyl Ru complexes has been rationalized in terms of a metal-based oxidation and a series of reductions

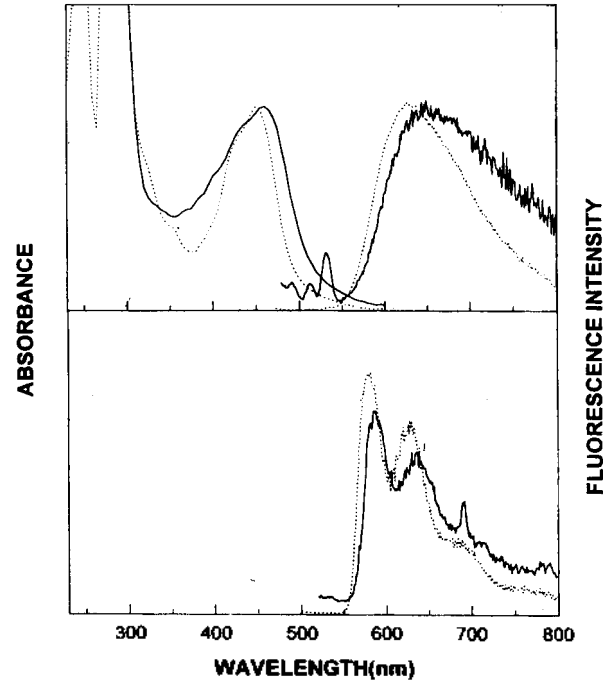

Figure 6. Absorption (left) and fluorescence (right) spectra of [Ru(bpy)$_2$(t-aemb)](PF$_6$)$_2$ (solid line) and [Ru(bpy)$_3$](PF$_6$)$_2$ (dotted line) in acetonitrile at room temperature (upper) in ethanol at 77 K (lower).

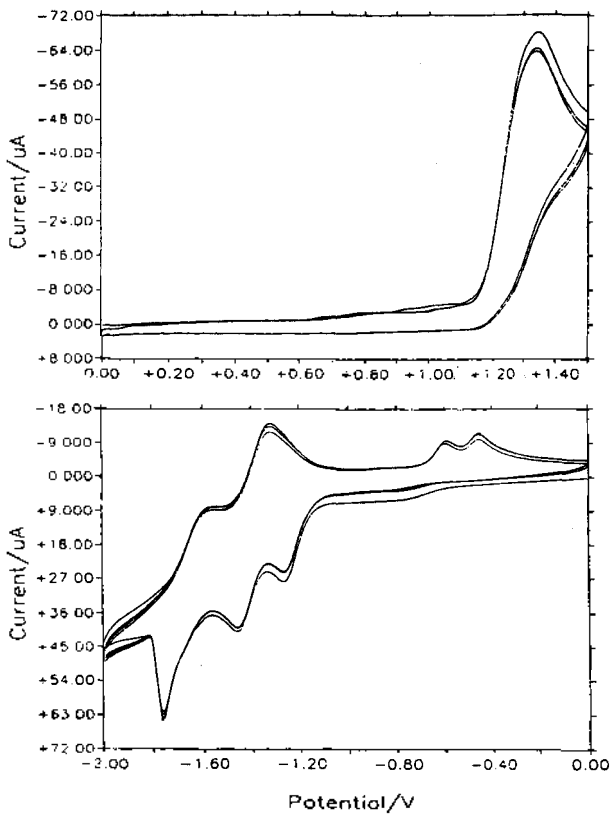

Figure 7. Cyclic voltammogram of $[Ru(bpy)_2(t\text{-aemb})](PF_6)_2$ in acetonitrile.

which are ligand-based. Electrochemical properties of $[(Ru(bpy)_2(t\text{-aemb})](PF_6)_2$ are collected in Table 2, together with the data for the reference Ru complexes for comparison.[5,6,13] As shown in Figure 7, irreversible oxidation of Ru^{II}/Ru^{III} is observed and the return wave in ligand-based reduction of -1.68 V is not smooth but becomes abruptly steep in the cyclic voltammogram. It is tentatively inferred that t-aemb undergoes electron-transfer catalized reaction, *e.g.* isomerization to c-aemb. It has been known that the *cis-trans* photoisomerization of some diarylethenes was sensitized by $[Ru(bpy)_3]^{2+}$ complex.[20]

Photolysis of $[(Ru(bpy)_2(t\text{-aemb})](PF_6)_2$. The absorption spectral changes of $[(Ru(bpy)_2(t\text{-aemb})](PF_6)_2$ in acetonitrile on irradiation of 350 nm (Figure 8) and 450 nm (Figure 9) were studied in order to investigate whether the photoinduced *trans*→*cis* isomerization of t-aemb ligand coordinated in $[(Ru(bpy)_2(t\text{-aemb})](PF_6)_2$ can occur as in free ligand or not. Continuous irradiation of $[(Ru(bpy)_2(t\text{-aemb})](PF_6)_2$ causes significant change in the absorption spectrum. On excitation of 350 nm into the band corresponding to absorption of t-aemb moiety, 288 nm band corresponding to bpy ligand-centered π-π^* transitions is nearly unchanged, but intensities of the 461 nm band of MLCT (d-π^*) transitions and the 254 nm band of t-aemb ligand-centered π-π^* transitions are decreased as shown in Figure 8. It is tentatively inferred that direct absorption by t-aemb leads to some photoreaction, e.g. photoisomerization of t-aemb to c-aemb. It agrees with the observation that $[(Ru(bpy)_2(t\text{-aemb})](PF_6)_2$ in acetonitrile shows no fluorescence at the excitation wavelength of 360 nm while weak

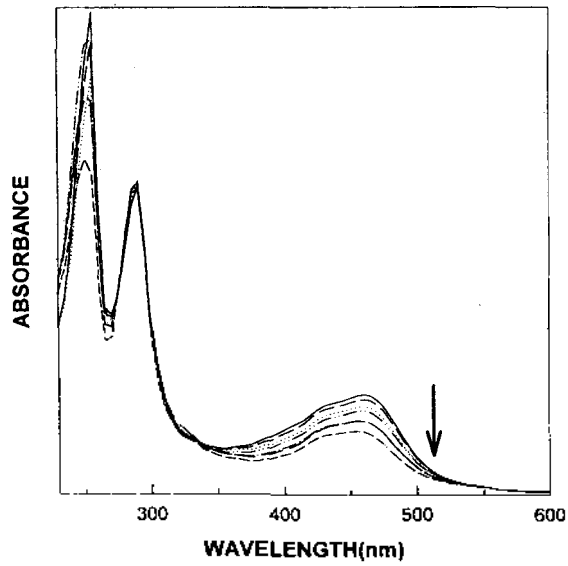

Figure 8. Absorption spectral changes of $[Ru(bpy)_2(t\text{-aemb})](PF_6)_2$ in acetonitrile in the interval of 10 min. on irradiation for 1 hr at 350 nm.

fluorescence is observed at the excitation wavelength of 460 nm. When the complex is irradiated at 450 nm, the absorption spectral change is somewhat different. Intensity of 288 nm band is also decreased with the marked reduction of 461 and 254 nm bands as shown in Figure 9. Irradiation of 450 nm seems to lead to the structural change of the ligand t-aemb along with the decomposition of the complex.

Further investigation will be carried out for the detailed mechanism. $[(Ru(bpy)_2(t\text{-aemb})](PF_6)_2$ is suggested to behave in part a bichromophoric system. Intramolecular energy or electron transfer induces the change of the structure and properties of the complex. This is an interesting example containing the photoresponsive ligand.

Acknowledgement. We are grateful to Prof. Myeong Ho Pyo at Sunchon National University for the electro-

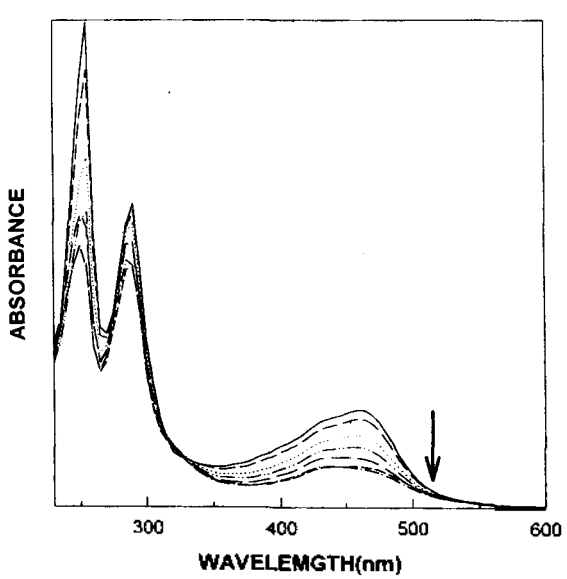

Figure 9. Absorption spectral change of $[Ru(bpy)_2(t\text{-aemb})](PF_6)_2$ in acetonitrile in the interval of 10 min. on irradiation for 1 hr at 450 nm.

chemical measurements and Prof. Taek Hyeon Kim and Prof. Jae Nyoung Kim at Chonnam National University for NMR measurements and Korea Basic Science Institute for fluorescence lifetime and FAB-mass spectral measurements.

References

1. Juris, A.; Balzani, V.; Barigelletti, F.; Campagna, S.; Belser, P.; Von Zelewsky, A. *Coord. Chem. Rev.* **1988,** *84*, 85.
2. Kalyanasundaram, K. *Coord. Chem. Rev.* **1982,** *46*, 159.
3. Balzani, V.; Juris, A.; Venturi, M.; Campagna, S.; Serroni, S. *Chem. Rev.* **1996,** *96*, 759.
4. Treadway, J. A.; Barbara, L.; Lopez, R.; Anderson, P. A.; Keene, F. R.; Meyer, T. J. *Inorg. Chem.* **1996,** *35*, 2242.
5. Strouse, G. F.; Schoonover, J. R.; Duesing, R.; Boyde, S.; Jones, Jr., W. E.; Meyer, T. J. *Inorg. Chem.* **1995,** *34*, 473.
6. Anderson, P. A.; Deacon, G. B.; Haarmann, K. H.; Keene, F. R.; Meyer, T. J.; Reitsma, D. A.; Skelton, B. W.; Strouse, G. F.; Thomas, N. C.; Treadway, J. A.; White, A. H. *Inorg. Chem.* **1995,** *34*, 6145.
7. Meyer, T. J. *Pure and Appl. Chem.* **1986,** *58*, 1576.
8. Kober, E. M.; Caspar, J. V.; Lumpkin, R. S.; Meyer, T. J. *J. Phys. Chem.* **1986,** *90*, 3722.
9. Sauvage, J.-P.; Collin, J. P.; Chambron, J. C.; Guillerez, S.; Coudret, C.; Balzani, V.; Barigelletti, F.; De Colar, L.; Flamigni, L. *Chem. Rev.* **1994,** *94*, 993.
10. Kelly, L. A.; Rodgers, M. A. *J. Phys. Chem.* **1995,** *99*, 13132.
11. Xu, X.; Shreder, K.; Iverson, B.; Bard, A. J. *J. Am. Chem. Soc.* **1996,** *118*, 3656.
12. Ciana, L. D.; Hamachi, I.; Meyer, T. J. *J. Org. Chem.* **1989,** *54*, 1731.
13. Weinheimer, C.; Choi, Y.; Caldwell, T.; Gressham, P.; Olmsted III, J. *J. Photochem. Photobiol. A: Chem.* **1994,** *78*, 119.
14. Sprintschnik, G.; Sprintschnik, H. W.; Kirsch, P. P.; Whitten, D. G. *J. Am. Chem. Soc.* **1977,** *99*, 4947.
15. Bartocci, G.; Masetti, F.; Mazzucato, U.; Spalletti, A.; Orlandi, G.; Poggi, G. *J. Chem. Soc., Faraday Trans. 2* **1988,** *84*, 385.
16. Aloisi, G. G.; Elisei, F.; Latterini, L.; Passerini, M.; Galiazzo, G. *J. Chem. Soc., Faraday Trans.* **1996,** *92*, 3315.
17. Shin, E. J.; Bae, E. Y.; Kim, S. H.; Kang, H. K.; Shim, S. C. *J. Photochem. Photobiol. A: Chem.* **1997,** *107*, 137.
18. Sun, L.; Gorner, H. *J. Phys. Chem.* **1993,** *97*, 11186.
19. Gorner, H. *J. Photochem. Photobiol. A: Chem.* **1988,** *43*, 263.
20. Takagi, K.; Ogata, Y. *J. Org. Chem.* **1982,** *47*, 1409.

Molecular Structure and Vibrational Spectra of Biphenyl in the Ground and the Lowest Triplet States. Density Functional Theory Study

Sang Yeon Lee

Department of Industrial Chemistry, Kyungpook National University, Taegu 702-701, Korea
Received September 24, 1997

The molecular geometries and harmonic vibrational frequencies of biphenyl in the ground and the first excited triplet states have been calculated using the Hartree-Fock and Becke-3-Lee-Yang-Parr (B3LYP) density functional methods with 6-31G* basis set. Structural change occurs from a twisted benzene-like to a planar quinone-like form upon the excitation to the first excited state. Scaled harmonic vibrational frequencies for the ground state obtained from the B3LYP calculation show good agreement with the available experimental data. A few vibrational fundamentals for both states are newly assigned based on the B3LYP results.

Introduction

Biphenyl (BP) and its derivatives have been extensively studied experimentally[1-14] and theoretically[15-18] to investigate the molecular structure and the spectroscopic properties. Recently, Sasaki and Hamaguchi recorded the transient resonance Raman spectra of BP and its perdeuterated one(BP-d_{10}) in the first excited triplet state and suggested that BP in the first excited triplet state takes a planar structure.[3] To assign peaks in the Raman spectra and confirm their suggestion, it is necessary to perform the complete vibrational analysis for BP in the ground and the first triplet states. The complete vibrational analysis for BP in the ground state will be very useful for the interpretation of the vibronic structures in the absorption and fluorescence spectra. Although the symmetry assignments of observed vibrational frequencies of BP in the ground state by Zerbi and Sandroni (ZS)[10] and by Bree, Pang and Rabeneck (BPR)[11] on the basis of the polarized infrared and Raman spectra are very excellent, their selection of fundamental frequencies from the complicated infrared and Raman spectra is not complete, and has some ambiguities because the selection was done based on the force field calculation and the assumption that the fundamental modes show the most intense bands in the spectra.